

## Six-point gluon scattering amplitudes from $\mathbb{Z}_4$ -symmetric integrable model

Yasuyuki Hatsuda\*, Katsushi Ito<sup>†</sup>, Kazuhiro Sakai<sup>‡</sup> and Yuji Satoh<sup>§</sup>

*\*Yukawa Institute for Theoretical Physics, Kyoto University  
Kyoto 606-8502, Japan*

*†Department of Physics, Tokyo Institute of Technology  
Tokyo 152-8551, Japan*

*‡Research and Education Center for Natural Sciences  
and Hiyoshi Department of Physics, Keio University  
Yokohama 223-8521, Japan*

*§Institute of Physics, University of Tsukuba  
Ibaraki 305-8571, Japan*

### Abstract

We study six-point gluon scattering amplitudes in  $\mathcal{N} = 4$  super Yang–Mills theory at strong coupling by investigating the thermodynamic Bethe ansatz equations of the underlying  $\mathbb{Z}_4$ -symmetric integrable model both analytically and numerically. By the conformal field theory (CFT) perturbation, we compute the free energy part of the remainder function with generic chemical potential near the CFT/small mass limit. Combining this with the expansion of the Y-functions, we obtain the remainder function near the small mass limit up to a function of the chemical potential, which can be evaluated numerically. We also find the leading corrections to the remainder function near the large mass limit. We confirm that these results are in good agreement with numerical computations.

May 2010

---

\*hatsuda@yukawa.kyoto-u.ac.jp

†ito@th.phys.titech.ac.jp

‡sakai@phys-h.keio.ac.jp

§ysatoh@het.ph.tsukuba.ac.jp

## 1. Introduction

Recently there has been much progress in computing the area of minimal surfaces in AdS space, whose boundary is made of light-like segments [1–7]. The surface area corresponds to the expectation value of the Wilson loop along the same contour and is dual to the gluon scattering amplitude in planar  $\mathcal{N} = 4$  super Yang–Mills theory at strong coupling. The minimal surface area has deviation from the Bern–Dixon–Smirnov (BDS) conjecture [8] by an amount of the remainder function, which is shown to exist for the  $n(\geq 6)$ -point amplitudes [9, 10]. Determination of the remainder function is a key step toward establishing the correct analytic formula of the gluon scattering amplitude.

In [3], the equations for determining the minimal surface in AdS<sub>5</sub> space are shown to be the SU(4) Hitchin equations with certain constraints and boundary conditions. The area is characterized by the Stokes data of the asymptotic solutions of the associated linear system. The Stokes data obey certain functional equations and the minimal surface area is evaluated by solving the integral equations associated with them. For the 6-point gluon scattering amplitudes, the functional equations and the integral equations turn out to be the Y-system [11] and the thermodynamic Bethe ansatz (TBA) equations [12] of the  $\mathbb{Z}_4$ -symmetric (or  $A_3$ ) integrable model [13–15], respectively. The minimal surface area is evaluated by the free energy of the model.

This solution has been generalized to the minimal surface with an  $n$ -sided light-like polygonal boundary in AdS<sub>5</sub> [5] and in AdS<sub>3</sub> [5, 6]. In particular, Alday, Maldacena, Sever and Vieira proposed the Y-system and the TBA equations for the  $n$ -sided polygonal solution and expressed the area in terms of the TBA system. In [6], the present authors noticed that the TBA system is that of the homogeneous sine-Gordon model [16].

The free energy for a two-dimensional integrable model with purely elastic S-matrix is obtained by solving the TBA system. It is very difficult to solve the TBA system exactly but one can investigate its solutions in two limits. In the UV (or high temperature or small mass) limit, it is described by a certain conformal field theory (CFT). In the IR (or low temperature or large mass) limit, on the other hand, it becomes a system of a free massive theory. In the UV limit, the free energy turns out to be the central charge of the CFT. In the case of the homogeneous sine-Gordon model, the relevant CFTs are the generalized parafermion CFTs [17]. A particularly interesting feature of the TBA system is that it contains chemical potential which arises from the monodromy of the asymptotic solution of the linear system. Its

solution with chemical potential near the CFT point has not been well studied.

While analysis in the above described limits reveals several principal characters of the amplitude, evaluation of the remainder function apart from the limits is also of great significance in studying how the amplitude depends on the gluon momenta. The purpose of this paper is to analyze such momenta dependence of the remainder function. To do this, we investigate the TBA system perturbatively both near the UV and IR limits. In the present work we will focus on the 6-point amplitude for simplicity, where the relevant CFT is the  $\mathbb{Z}_4$ -parafermion CFT. The solution of the TBA system without chemical potential around the CFT point was studied by Klassen and Melzer [18]. In this paper we will investigate the perturbative solution around the CFT point including chemical potential. We also study the TBA system near the IR limit and present the first correction to the remainder function.

Our results provide an analytic form of the remainder function for the 6-point scattering amplitude at strong coupling away from the CFT and the IR point. This paper also demonstrates that the unexpected connection between the four-dimensional super Yang–Mills theory and the two-dimensional integrable models discovered in [3, 6] enables one to compute the amplitude at strong coupling in two-dimensional approaches. From a point of view of the study of integrable models, our discussion provides a concrete example of an analysis of TBA systems with chemical potential.

This paper is organized as follows. In sect. 2, we review the construction of the Hitchin equations of the minimal surface with a 6-sided polygonal boundary in  $\text{AdS}_5$  and the related Y-system and TBA equations. In sect. 3, we study the CFT limit of the TBA system and evaluate the free energy perturbatively. In sect. 4, we study the remainder function around the CFT limit. In sect. 5, we examine the large mass limit and obtain the correction to the remainder function. We conclude with a discussion in sect. 6.

## 2. Review of TBA system for six-point amplitudes

In this section we review the TBA system for the six-point gluon scattering amplitudes. We basically follow the references [3, 5].

### 2.1. Classical string solutions with a null polygonal boundary

Alday and Maldacena proposed a method of computing gluon scattering amplitudes in  $\mathcal{N} = 4$  super Yang–Mills using AdS/CFT correspondence [1]. According to their

proposal, scalar magnitude of  $n$ -gluon MHV scattering amplitudes can be evaluated in the strong coupling limit by computing the area of corresponding classical open string solutions. The string solutions are minimal surfaces whose boundary is a polygon located on the boundary of  $AdS_5$ . The polygon consists of  $n$  null edges given by the  $n$  momenta of incoming gluons.

To be concrete, classical string solutions under consideration are realized as a map from their world-sheet to  $AdS_5$ . We consider Euclidean world-sheet parametrized by  $z, \bar{z}$ . In terms of the global coordinates,  $AdS_5$  is expressed as a hypersurface

$$\vec{X} \cdot \vec{X} \equiv -(X^{-1})^2 - (X^0)^2 + (X^1)^2 + (X^2)^2 + (X^3)^2 + (X^4)^2 = -1 \quad (2.1)$$

in  $\mathbb{R}^{2,4}$ . Classical string solutions  $\vec{X}(z, \bar{z})$  satisfy the equations of motion

$$\partial \bar{\partial} \vec{X} - (\partial \vec{X} \cdot \bar{\partial} \vec{X}) \vec{X} = 0 \quad (2.2)$$

and the Virasoro constraints

$$\partial \vec{X} \cdot \partial \vec{X} = \bar{\partial} \vec{X} \cdot \bar{\partial} \vec{X} = 0. \quad (2.3)$$

The boundary condition is expressed in terms of the Poincaré coordinates  $(r, x^\mu)$  given by

$$X^\mu = \frac{x^\mu}{r}, \quad \mu = 0, 1, 2, 3, \quad (2.4)$$

$$X^{-1} + X^4 = \frac{1}{r} \quad X^{-1} - X^4 = \frac{r^2 + x^\mu x_\mu}{r}. \quad (2.5)$$

The solutions which correspond to  $n$ -gluon amplitudes end on an  $n$ -sided polygon at the AdS boundary  $r = 0$ . The vertices  $x_1, \dots, x_n$  of the polygon are separated by the gluon momenta  $k_1, \dots, k_n$  as

$$x_j^\mu - x_{j+1}^\mu = k_j^\mu. \quad (2.6)$$

This type of boundary condition is neatly characterized in terms of the generalized sinh-Gordon potential [19]. Let us introduce the following notation

$$e^{\alpha(z, \bar{z})} = \partial \vec{X} \cdot \bar{\partial} \vec{X}, \quad (2.7)$$

$$P(z) = \partial^2 \vec{X} \cdot \partial^2 \vec{X}, \quad \bar{P}(\bar{z}) = \bar{\partial}^2 \vec{X} \cdot \bar{\partial}^2 \vec{X}, \quad (2.8)$$

$$\hat{\alpha}(z, \bar{z}) = \alpha(z, \bar{z}) - \frac{1}{4} \log P(z) \bar{P}(\bar{z}), \quad (2.9)$$

where  $\alpha, \hat{\alpha}$  are real and  $P(z)$  is shown to be analytic in  $z$ . For the simplest four-cusp solution,  $P(z) = 1$  and  $\hat{\alpha} = 0$  on the whole  $z$ -plane. For  $n$ -cusp solutions,  $P(z)$  is

a polynomial of degree  $n - 4$  and  $\hat{\alpha} \rightarrow 0$  for  $|z| \rightarrow \infty$ . The latter condition reflects the fact that  $n$ -cusp solutions have the same asymptotics with the four-cusp solution around each cusp.

In this paper we will concentrate on the case of  $n = 6$ , where  $P(z)$  is quadratic. One can choose a gauge

$$P(z) = z^2 - U, \quad U \in \mathbb{C} \quad (2.10)$$

by a suitable redefinition of the world-sheet coordinate.

## 2.2. Hitchin system

The equations of motion (2.2) and the Virasoro constraints (2.3) can be rephrased as SU(4) Hitchin equations [3]. To see this, let us consider a moving-frame basis spanned by  $\vec{q}_0 = \vec{X}$ ,  $\vec{q}_4 = e^{-\alpha/2} \partial \vec{X}$ ,  $\vec{q}_5 = e^{-\alpha/2} \bar{\partial} \vec{X}$  and the other three complementary orthonormal vectors  $\vec{q}_I$ ,  $I = 1, 2, 3$ . The evolution of the basis  $q = (\vec{q}_0, \dots, \vec{q}_5)$  is described by a set of linear differential equations

$$\partial q = -\mathcal{A}_z q, \quad \bar{\partial} q = -\mathcal{A}_{\bar{z}} q. \quad (2.11)$$

One can decompose the connection into two parts  $\mathcal{A} = A + \Phi$ , in such a way that  $A$  rotates  $(\vec{q}_0, \vec{q}_1, \vec{q}_2, \vec{q}_3)$  and  $(\vec{q}_4, \vec{q}_5)$  separately among themselves while  $\Phi$  mixes them. The flatness condition of (2.11) then takes the form of the Hitchin equations

$$D_z \Phi_{\bar{z}} = 0, \quad D_{\bar{z}} \Phi_z = 0, \quad (2.12)$$

$$[D_z, D_{\bar{z}}] + [\Phi_z, \Phi_{\bar{z}}] = 0, \quad (2.13)$$

where  $D_z = \partial + [A_z, \ ]$ ,  $D_{\bar{z}} = \bar{\partial} + [A_{\bar{z}}, \ ]$ . These equations are equivalent to the equations of motion (2.2) and the Virasoro constraints (2.3). One can write down the same equations in the spinor basis, where  $A_z, A_{\bar{z}}, \Phi_z, \Phi_{\bar{z}}$  now represent  $4 \times 4$  matrices. We do not need their explicit form [3] here, but an important fact is that these  $A$  and  $\Phi$  corresponding to string solutions satisfy additional constraints

$$CA^T C^{-1} = -A, \quad C\Phi^T C^{-1} = i\Phi, \quad (2.14)$$

with a certain constant matrix  $C$ . This leads to a  $\mathbb{Z}_4$  automorphism in the present Hitchin system. This  $\mathbb{Z}_4$  automorphism is not inherent in general Hitchin systems but is peculiar to the one describing the classical strings in  $AdS_5$ . The system also exhibits  $\mathbb{Z}_2$  automorphism that corresponds to the reality of the string solutions.

As argued above,  $n$ -cusp solutions are characterized by the condition that  $\hat{\alpha} \rightarrow 0$  for  $|z| \rightarrow \infty$ . This is equivalent to the statement that one can always diagonalize  $\Phi$  and  $A$  at large  $|z|$  by a suitable gauge transformation into the following form

$$h^{-1}\Phi_z h \rightarrow \frac{1}{\sqrt{2}} \begin{pmatrix} P(z)^{1/4} & & & \\ & -iP(z)^{1/4} & & \\ & & -P(z)^{1/4} & \\ & & & iP(z)^{1/4} \end{pmatrix}, \quad (2.15)$$

$$h^{-1}A_z h + h^{-1}\partial h \rightarrow \frac{m}{z} \begin{pmatrix} \sigma_3 & 0 \\ 0 & \sigma_3 \end{pmatrix}, \quad h^{-1}A_{\bar{z}} h + h^{-1}\bar{\partial} h \rightarrow -\frac{\bar{m}}{\bar{z}} \begin{pmatrix} \sigma_3 & 0 \\ 0 & \sigma_3 \end{pmatrix}, \quad (2.16)$$

where  $m$  and  $\bar{m}$  are constants.

### 2.3. Auxiliary linear problem and small solutions

The system under consideration is classically integrable. This means that the connections appeared in the linear equations can be promoted to a set of one-parameter family of flat connections. That is to say, one can write down an auxiliary linear problem

$$\nabla_z^\zeta q(z, \bar{z}; \zeta) = 0, \quad \nabla_{\bar{z}}^\zeta q(z, \bar{z}; \zeta) = 0, \quad (2.17)$$

with

$$\nabla_z^\zeta = D_z + \zeta^{-1}\Phi_z, \quad \nabla_{\bar{z}}^\zeta = D_{\bar{z}} + \zeta\Phi_{\bar{z}}, \quad (2.18)$$

where the Hitchin equations (2.12), (2.13) are obtained as the compatibility condition

$$[\nabla_z^\zeta, \nabla_{\bar{z}}^\zeta] = 0. \quad (2.19)$$

One can estimate the asymptotic form of the solutions  $q(z, \bar{z}; \zeta)$  for large  $|z|$ . There are four independent solutions, whose asymptotic forms are respectively given by

$$\vec{e}_1 z^m \bar{z}^{-\bar{m}} e^{\frac{1}{\sqrt{2}}(\zeta^{-1}w + \zeta\bar{w})}, \quad \vec{e}_2 z^{-m} \bar{z}^{\bar{m}} e^{-i}$$

We call such solution the small solution  $s_k(z, \bar{z}; \zeta)$  in the sector  $W_k$ . Small solutions form a set of redundant basis of the solutions to the equations (2.17). We normalize the solutions so that

$$\langle s_j, s_{j+1}, s_{j+2}, s_{j+3} \rangle = 1, \quad (2.22)$$

where  $\langle s_i, s_j, s_k, s_l \rangle \equiv \det(s_i s_j s_k s_l)$ . As the differential operators are regular everywhere in  $|z| < \infty$ , the sectors  $W_j$  and  $W_{j+n}$  are identified. Hence

$$s_{j+n} \propto s_j. \quad (2.23)$$

One can determine the proportionality coefficient case by case whether  $n = 2k - 1$ ,  $n = 4k - 2$  or  $n = 4k$  for  $k \in \mathbb{Z}_{>0}$ . In the case of  $n = 6$ ,

$$s_{j+6} = \mu^{(-1)^j} s_j \quad (2.24)$$

where

$$\mu = \pm e^{2\pi i(m + \bar{m})}. \quad (2.25)$$

Note that  $\mu$  is a pure phase factor for solutions in the usual (3, 1) signature. For later use, let us also introduce the notation

$$\mu = e^{i\phi} \quad (2.26)$$

with  $\phi$  being a real parameter.

## 2.4. Y-system

Making use of integrability, one can compute conserved quantities without knowing the explicit form of solutions. Instead, the fundamental building blocks are the Stokes data  $\langle s_i, s_j, s_k, s_l \rangle(\zeta)$ . Let us first recall some important identities concerning them. In addition to the normalization condition (2.22), there hold the following identities

$$\langle s_k, s_{k+1}, s_j, s_{j+1} \rangle(\zeta) = \langle s_{k-1}, s_k, s_{j-1}, s_j \rangle(i\zeta), \quad (2.27)$$

$$\langle s_j, s_k, s_{k+1}, s_{k+2} \rangle(\zeta) = \langle s_j, s_{j-1}, s_{j-2}, s_k \rangle(i\zeta), \quad (2.28)$$

which follow from the  $\mathbb{Z}_4$  automorphism.

In [5] Alday, Maldacena, Sever and Vieira formulated the T-system and the Y-system associated to the general  $n$ -cusp solutions in  $AdS_5$ . There, some particular Stokes data are chosen as T-functions and subsequently Y-functions are defined as

ratios of the form  $Y = TT/TT$ . Similar formulation of T- and Y-system was obtained from the spectral theory of ordinary differential equations [20]. By restricting ourselves to the  $n = 6$  case, which is the simplest nontrivial case in their formulation, general formulas partly get simplified due to the relation (2.22). Y-functions are then defined by<sup>1</sup>

$$Y_1(\theta) = -\langle s_2, s_3, s_5, s_6 \rangle (e^\theta), \quad (2.29)$$

$$Y_2(\theta) = \langle s_1, s_2, s_3, s_5 \rangle \langle s_2, s_4, s_5, s_6 \rangle (e^{\theta+\pi i/4}), \quad (2.30)$$

$$Y_3(\theta) = Y_1(\theta). \quad (2.31)$$

These Y-functions are not entirely independent, but satisfy functional relations. By using Hirota bilinear identities (or Plücker relations) among determinants and (2.24) (2.27), (2.28), one can show that

$$Y_1\left(\theta + \frac{\pi i}{4}\right) Y_1\left(\theta - \frac{\pi i}{4}\right) = 1 + Y_2(\theta), \quad (2.32)$$

$$Y_2\left(\theta + \frac{\pi i}{4}\right) Y_2\left(\theta - \frac{\pi i}{4}\right) = (1 + \mu Y_1(\theta))(1 + \mu^{-1} Y_1(\theta)). \quad (2.33)$$

Another important property of the Y-functions is the periodicity

$$Y_a\left(\theta + \frac{3\pi i}{2}\right) = Y_a(\theta), \quad (2.34)$$

which also follows from (2.24), (2.27), (2.28). They also satisfy

$$\overline{Y_a(\theta)} = Y_a(-\bar{\theta}), \quad (2.35)$$

which follows from the reality of string solutions.

In fact, the Y-system obtained here is identified with that [11] of  $\mathbb{Z}_N$ -symmetric integrable models [13–15] with  $N = 4$ .  $Y_a$  correspond to the fundamental representations labeled by  $a = 1, 2, 3$  of the  $A_3$  Lie algebra. The present Y-system corresponds to the model with a chemical potential  $\mu$  turned on. Note that the periodicity (2.34) holds in the presence of  $\mu$ .

The cross-ratios of gluon momenta are given by special values of the Y-functions,

$$b_k = Y_1\left(\frac{(k-1)\pi i}{2}\right), \quad U_k = 1 + Y_2\left(\frac{(2k+1)\pi i}{4}\right), \quad (2.36)$$

---

<sup>1</sup> Y-functions introduced here are identified with those in [5] as  $Y_1(\theta) = \mu^{-1}[Y_{1,1}^{\text{AMSV}}(ie^\theta)]^{-1}$ ,  $Y_2(\theta) = [Y_{2,1}^{\text{AMSV}}(ie^\theta)]^{-1}$ ,  $Y_3(\theta) = \mu[Y_{3,1}^{\text{AMSV}}(ie^\theta)]^{-1}$ .



for  $k = 1, 2, 3$ , where

$$U_1 = b_2 b_3 = \frac{x_{14}^2 x_{36}^2}{x_{13}^2 x_{46}^2}, \quad U_2 = b_3 b_1 = \frac{x_{25}^2 x_{14}^2}{x_{24}^2 x_{15}^2}, \quad U_3 = b_1 b_2 = \frac{x_{36}^2 x_{25}^2}{x_{35}^2 x_{26}^2}. \quad (2.37)$$

From the Y-system relations (2.32), (2.33) one can verify that  $b_j$ 's are not entirely independent but obey the constraint

$$b_1 b_2 b_3 = b_1 + b_2 + b_3 + \mu + \mu^{-1}. \quad (2.38)$$

## 2.5. TBA equations

The functional relations described above constrain the form of Y-functions mostly, but not entirely. To fully determine the Y-functions, we need an additional information such as the asymptotic behavior and the singularity structure. The asymptotic behavior of the Y-functions can be evaluated by the WKB analysis [21]. It can be shown that the Y-functions defined by (2.29)–(2.31) exhibit the following asymptotics

$$\begin{aligned} \log Y_1(\theta) &\rightarrow |Z| e^{\pm(\theta - i\varphi)}, & \log Y_2(\theta) &\rightarrow \sqrt{2} |Z| e^{\pm(\theta - i\varphi)} \\ \text{for } \operatorname{Re} \theta &\rightarrow \pm\infty, & \varphi - \frac{\pi}{4} &< \operatorname{Im} \theta < \varphi + \frac{\pi}{4}, \end{aligned} \quad (2.39)$$

where  $Z$  is related to the moduli parameter  $U$  in (2.10) as

$$Z \equiv |Z| e^{i\varphi} = U^{\frac{3}{4}} \int_{-1}^1 (1 - t^2)^{\frac{1}{4}} dt = \frac{\sqrt{\pi} \Gamma(\frac{1}{4})}{3\Gamma(\frac{3}{4})} U^{\frac{3}{4}}. \quad (2.40)$$

As for the singularity structure, one can take Y-functions regular everywhere except at  $\operatorname{Re} \theta = \pm\infty$ . This is consistent with the functional relations (2.32), (2.33). One could also consider Y-functions with singularities at finite  $\theta$ . These correspond to excited states. Since we are interested in minimal area surfaces which correspond to the ground state, we restrict ourselves to the Y-functions regular at finite  $\theta$ .

Taking these into account, one can write down a set of integral equations which fully determine the form of Y-functions. By introducing the following notations

$$\epsilon(\theta) = \log Y_1(\theta + i\varphi), \quad \tilde{\epsilon}(\theta) = \log Y_2(\theta + i\varphi), \quad (2.41)$$

the integral equations can be written in the form of TBA equations

$$\epsilon = 2|Z| \cosh \theta + \mathcal{K}_2 * \log(1 + e^{-\tilde{\epsilon}}) + \mathcal{K}_1 * \log(1 + \mu e^{-\epsilon})(1 + \mu^{-1} e^{-\epsilon}), \quad (2.42)$$

$$\tilde{\epsilon} = 2\sqrt{2}|Z| \cosh \theta + 2\mathcal{K}_1 * \log(1 + e^{-\tilde{\epsilon}}) + \mathcal{K}_2 * \log(1 + \mu e^{-\epsilon})(1 + \mu^{-1} e^{-\epsilon}), \quad (2.43)$$

where

$$\mathcal{K}_1(\theta) = \frac{1}{2\pi \cosh \theta}, \quad \mathcal{K}_2(\theta) = \frac{\sqrt{2} \cosh \theta}{\pi \cosh 2\theta}, \quad (2.44)$$

and  $f * g = \int_{-\infty}^{\infty} d\theta' f(\theta - \theta')g(\theta')$ . Note that these equations are valid in the strip region  $-\pi/4 < \text{Im } \theta < \pi/4$ . From these equations it is clear that  $\epsilon(\theta), \tilde{\epsilon}(\theta)$  are even, real functions

$$\epsilon(-\theta) = \epsilon(\theta), \quad \tilde{\epsilon}(-\theta) = \tilde{\epsilon}(\theta), \quad (2.45)$$

$$\overline{\epsilon(\theta)} = \epsilon(\bar{\theta}), \quad \overline{\tilde{\epsilon}(\theta)} = \tilde{\epsilon}(\bar{\theta}). \quad (2.46)$$

In terms of Y-functions, these properties are expressed as

$$Y_a(-\theta + i\varphi) = Y_a(\theta + i\varphi) \quad (2.47)$$

and (2.35).

Historically, the above TBA equations were first constructed for the  $\mathbb{Z}_4$ -symmetric integrable model. Indeed, the integral kernels can be obtained as derivatives of logarithm of the S-matrix elements in the  $\mathbb{Z}_N$  model [13] with  $N = 4$ .

By using (2.36), the cross-ratios (2.37) are expressed in terms of  $\epsilon(\theta), \tilde{\epsilon}(\theta)$ . If one wants to keep  $\epsilon, \tilde{\epsilon}$  evaluated within the above strip region, the appropriate choice of formulas are

$$b_{k+1} = \exp \left[ \epsilon \left( \frac{k\pi i}{2} - i\varphi \right) \right], \quad U_{k-1} = 1 + \exp \left[ \tilde{\epsilon} \left( \frac{(2k-1)\pi i}{4} - i\varphi \right) \right] \quad (2.48)$$

for  $(2k-1)\pi/4 < \varphi < k\pi/2$ , and

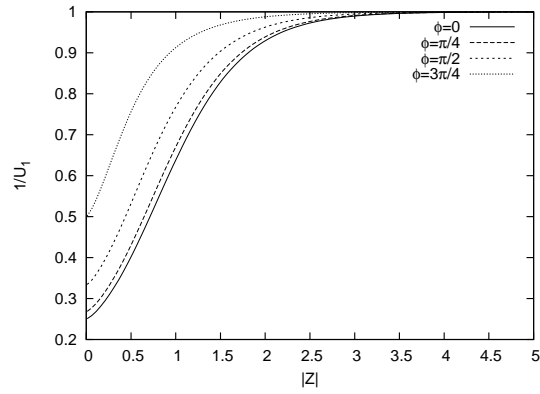
$$b_{k+1} = \exp \left[ \epsilon \left( \frac{k\pi i}{2} - i\varphi \right) \right], \quad U_k = 1 + \exp \left[ \tilde{\epsilon} \left( \frac{(2k+1)\pi i}{4} - i\varphi \right) \right] \quad (2.49)$$

for  $k\pi/2 < \varphi < (2k+1)\pi/4$ , where  $k = 1, 2, 3 \pmod{3}$ . The other cross-ratios are obtained by solving the relations (2.37) and (2.38).

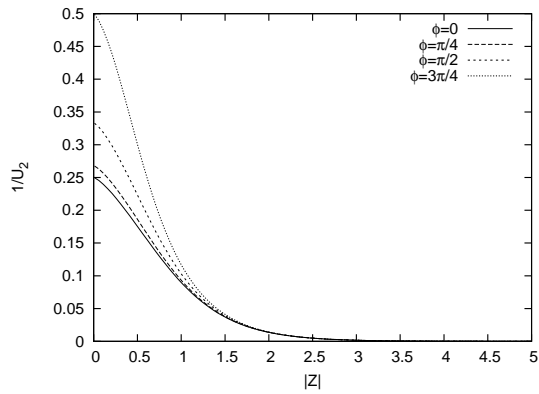
Solving the TBA equations numerically, we can calculate the cross-ratios as functions of  $|Z|$ ,  $\varphi$  and  $\phi$ . In Figure 1, we plot  $1/U_k$  for various  $\phi$  at fixed  $\varphi = -\pi/48$  as an example.<sup>2</sup>

---

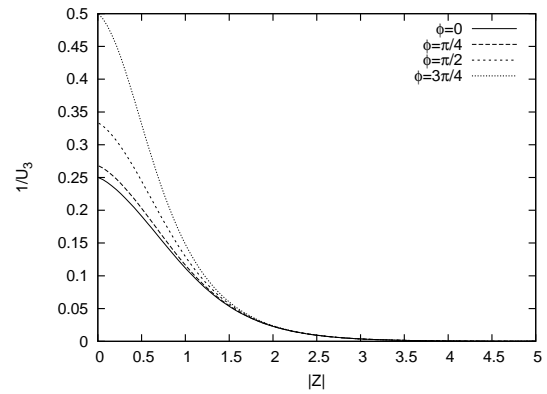
<sup>2</sup>  $\varphi = -\pi/48$  is merely a generic value and does not have particular meaning.



(a)



(b)



(c)

Figure 1: (a) The  $|Z|$ -dependence of the function  $1/U_1$  for different values of  $\phi$  at  $\varphi = -\pi/48$ . (b)  $1/U_2$ . (c)  $1/U_3$ .

## 2.6. Area and remainder function

As explained in [3, 5] in detail, the area of general  $n$ -cusp solutions with  $n \neq 4k$  ( $k \in \mathbb{Z}_{>0}$ ) can be written as<sup>3</sup>

$$A = A_{\text{div}} + A_{\text{BDS-like}} + A_{\text{periods}} + A_{\text{free}} + \text{const.} \quad (2.50)$$

$A_{\text{div}}$  and  $A_{\text{BDS-like}}$  are contributions from the region inside the AdS radial coordinate cut-off and can be evaluated for general  $n$ .  $A_{\text{periods}}$  is given by a period integral over the Riemann surface of the  $w$ -coordinate defined by  $dw = P(z)^{1/4} dz$ .  $A_{\text{free}}$  is shown to be identified with (minus) the free energy of the TBA system.

On the other hand, there is known an all-order ansatz for the MHV gluon scattering amplitudes proposed by Bern, Dixon and Smirnov [8]. It was shown (assuming the dual conformal symmetry) that BDS ansatz is correct for  $n = 4, 5$ , but deviates from the string theory computation for  $n \geq 6$  [9]. The function which complements the ansatz to produce the full gluon scattering amplitude is called the remainder function  $R$ . In the strong coupling limit, scalar magnitude of gluon scattering amplitudes is then expressed as

$$-A = -A_{\text{div}} - A_{\text{BDS}} + R. \quad (2.51)$$

$A_{\text{div}}$  is identical to that in the string theory computation, with appropriate identification of the cut-off parameters.  $A_{\text{BDS}}$  can be computed from one-loop perturbation and is known for general  $n$ .

Taken altogether, the remainder function in the strong coupling limit is expressed as

$$\begin{aligned} R &= A_{\text{BDS}} - A_{\text{BDS-like}} - A_{\text{periods}} - A_{\text{free}} + \text{const.} \\ &= R_1 - A_{\text{periods}} - A_{\text{free}} + \text{const.}, \end{aligned} \quad (2.52)$$

where

$$R_1 \equiv A_{\text{BDS}} - A_{\text{BDS-like}}. \quad (2.53)$$

Below we drop the constant term in (2.52).

---

<sup>3</sup> For  $n = 4k$  ( $k \in \mathbb{Z}_{>0}$ ) one needs extra terms [5, 7].

In the case of  $n = 6$ , terms in (2.52) are explicitly given by<sup>4</sup>

$$R_1 = -\frac{1}{4} \sum_{k=1}^3 \text{Li}_2(1 - U_k), \quad (2.54)$$

$$A_{\text{periods}} = |Z|^2, \quad (2.55)$$

$$-F = A_{\text{free}} = \frac{1}{2\pi} \int_{-\infty}^{\infty} d\theta \left( 2|Z| \cosh \theta \log(1 + \mu e^{-\epsilon(\theta)}) (1 + \mu^{-1} e^{-\epsilon(\theta)}) \right. \\ \left. + 2\sqrt{2}|Z| \cosh \theta \log(1 + e^{-\tilde{\epsilon}(\theta)}) \right). \quad (2.56)$$

Figure 2 and 3 show numerical results of the free energy and the remainder function at  $\varphi = -\pi/48$  respectively, where the value of  $\varphi$  is the same as in Figure 1. From Figure 1 and 3(b), we can read off the value of the remainder functions as the functions of the cross-ratios  $U_k$ .

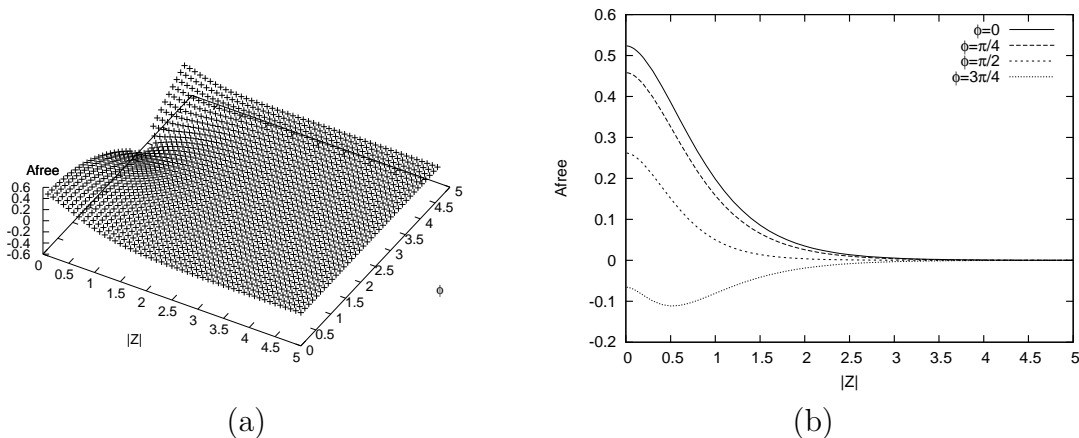


Figure 2: (a) 3D plots of free energy  $A_{\text{free}}$  as a function of  $|Z|$  and  $\phi$  ( $0 \leq |Z| \leq 5$ ,  $0 \leq \phi \leq 3\pi/2$ ) at  $\varphi = -\pi/48$ . (b)  $|Z|$ - $A_{\text{free}}$  graphs for various values of  $\phi$  at  $\varphi = -\pi/48$ .

Let us comment on choice of variables. General  $n$ -point gluon scattering amplitudes have  $3n - 15$  real moduli degrees of freedom. Correspondingly in the present case, the remainder function  $R$  for six-point amplitudes is a function of three independent real parameters. One can express  $R$ , either as a function of the momentum cross-ratios  $U_k$  or as a function of the moduli parameters  $|Z|, \varphi, \phi$ . The former choice respects the point of view of the four-dimensional  $\mathcal{N} = 4$  gauge theory while the latter fit well with the two-dimensional description. In the following sections we mainly

<sup>4</sup> In [3]  $R_1$  is expressed as  $R_1 = \sum_{k=1}^3 \left( \frac{1}{8} \log^2 u_k + \frac{1}{4} \text{Li}_2(1 - u_k) \right)$  with  $u_k = U_k^{-1}$ . This can be rewritten as in (2.54) for  $u_k \notin (-\infty, 0)$  by using a dilogarithm identity.

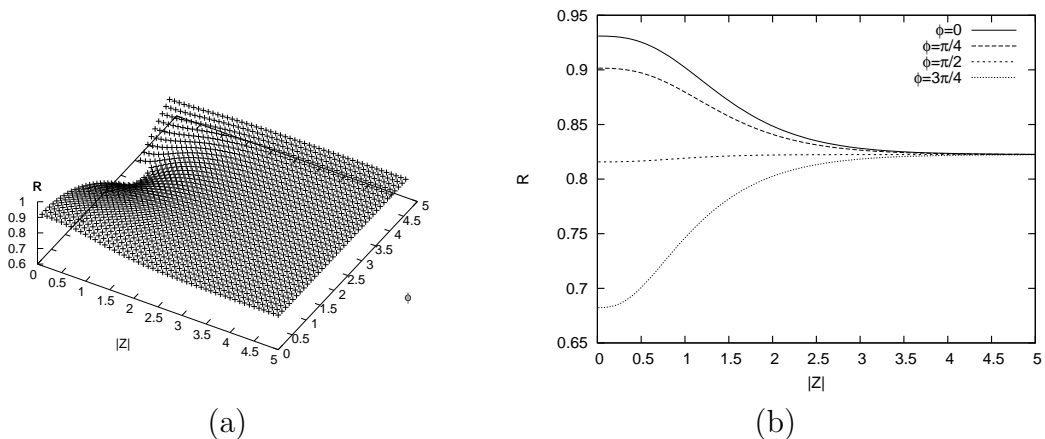


Figure 3: (a) 3D plots of numerical data of remainder function  $R$  as a function of  $|Z|$  and  $\phi$  at  $\varphi = -\pi/48$ . (b)  $|Z|$ - $R$  graphs for various values of  $\phi$  at  $\varphi = -\pi/48$ .

adopt the latter picture and study functional properties of  $R$  as well as its constituents  $A_{\text{free}}$  and  $R_1$ , in particular in the two extreme regions  $|Z| \ll 1$  and  $|Z| \gg 1$ . The former picture in terms of the cross-ratios is also discussed.

### 3. Free energy around CFT point

The TBA equations describing the six-point gluon scattering amplitudes (2.42)–(2.43) result from minimizing the free energy of the two-dimensional  $\mathbb{Z}_4$ -symmetric integrable field theory [18], which is obtained by deforming the  $\mathbb{Z}_4$  parafermion CFT [17] by the first energy operator [14, 15]. The model contains three particles with mass  $m$ ,  $\sqrt{2}m$  and  $m$ , respectively. The third one is the anti-particle of the first. The free energy of the model on a space of length  $L \gg 1$  with temperature  $1/R$  gives the ground state energy of the model on a space of length  $R$  [12]. The TBA equations (2.42)–(2.43) tell us that the scale  $R$  is related to  $|Z|$  as  $mR = 2|Z|$ . In [3], the free energy and the regularized area in the CFT limit  $mR \rightarrow 0$  are analyzed. In this limit, the cross-ratios take the values on the locus  $U_1 = U_2 = U_3$ . In this section, we discuss the corrections to the free energy around the CFT point.

We begin by noting that the action of the integrable model takes the form

$$S = S_{\text{PF}} + \lambda \int d^2x \varepsilon(x). \quad (3.1)$$

Here,  $S_{\text{PF}}$  is the action of the  $\mathbb{Z}_4$  parafermion CFT, and  $\varepsilon$  is the canonically normalized first energy operator with conformal dimension  $D_\varepsilon = \bar{D}_\varepsilon = 1/3$ . The coupling

constant  $\lambda > 0$  is related to the mass  $m$  as [22]

$$(2\pi\lambda)^2 = \left[ m\sqrt{\pi} \gamma\left(\frac{3}{4}\right) \right]^{\frac{8}{3}} \gamma\left(\frac{1}{6}\right), \quad (3.2)$$

where  $\gamma(x) \equiv \Gamma(x)/\Gamma(1-x)$ .

The free energy around the CFT point is then given by the ground state energy  $E(R)$  of the perturbed CFT on a cylinder of circumference  $R$  with small  $\lambda$  in (3.1) [12].<sup>5</sup>

$$F = RE(R) - R^2 B(\lambda), \quad (3.3)$$

where  $E(R)$  is expanded by the connected CFT correlators as

$$E(R) = E_0 - R \sum_{n=1}^{\infty} \frac{(-\lambda)^n}{n!} \left(\frac{2\pi}{R}\right)^{2(D_\varepsilon-1)n+2} \times \int \left\langle V(\infty) \varepsilon(z_n, \bar{z}_n) \cdots \varepsilon(z_1, \bar{z}_1) V(0) \right\rangle_{\text{connected}} \prod_{i=2}^n (z_i \bar{z}_i)^{D_\varepsilon-1} dz_i^2. \quad (3.4)$$

In the above,  $E_0$  is the unperturbed ground state energy,  $V$  is the operator corresponding to the vacuum, and the correlators are evaluated on the complex plane after a conformal transformation from the cylinder. We have also set  $z_1 = \bar{z}_1 = 1$ . Substituting  $\lambda$  in (3.2), one finds that the ground state energy has an expansion in  $(mR)^{\frac{4}{3}n}$ . Due to the  $\mathbb{Z}_2$  symmetry  $\varepsilon \rightarrow -\varepsilon$ , only the terms with even  $n$  remain in the expansion [18].

The second term in (3.3) subtracts the bulk contribution to  $E(R)$ , so that the free energy per unit length vanishes at zero temperature  $R \rightarrow \infty$  as implied by (2.56) and the TBA equations. This term is evaluated as [18]

$$B(\lambda) = -\frac{1}{4}m^2. \quad (3.5)$$

Although the derivation in [18] is given for  $\mu = 1$ , the asymptotics needed there may hold also for  $\mu \neq 1$  to give the same result. We will confirm that (3.5) is in agreement with the numerical results for both  $\mu = 1$  and  $\mu \neq 1$ .

Without the chemical potential, namely, for  $\mu = 1$ , the vacuum operator  $V$  is the identity, and thus the expansion is straightforward. To proceed in the case with general  $\mu$ , we recall the connection between the  $\mathbb{Z}_4$  parafermion model and the spin- $\frac{1}{2}$  XXZ (XXZ<sub>1/2</sub>) model, the Hamiltonian of which is

$$H_{XXZ} = \sum_{j=1}^N \left[ S_j^x S_{j+1}^x + S_j^y S_{j+1}^y + \cos \alpha S_j^z S_{j+1}^z \right]. \quad (3.6)$$

---

<sup>5</sup> We have rescaled the free energy as  $R^2 F/L \rightarrow F$  in accord with (2.56).

In the continuum limit, the spin variables are represented by a free boson  $\Phi(\tau, \sigma)$  [23]:

$$\begin{aligned} S_j^z &\sim \frac{1}{2\pi r} \partial_\sigma \Phi + (-1)^j c_1 \cos(\Phi/r), \\ S_j^- &\sim e^{\frac{i}{2} r \tilde{\Phi}} \left[ c_2 \cos(\Phi/r) + (-1)^j c_3 \right], \end{aligned} \quad (3.7)$$

where  $S_j^\pm \equiv S_j^x \pm i S_j^y$ ,  $c_a$  are constants,  $\tilde{\Phi}$  is the dual boson, and  $(\tau, \sigma)$  are the two-dimensional coordinates.  $r$  is the compactification radius, *i.e.*,  $\Phi \sim \Phi + 2\pi r$ , and is related to the coupling constant by  $r = \sqrt{2(1 - \frac{\alpha}{\pi})}$  [24] in the unit where the selfdual radius is  $r_{\text{sd}} = \sqrt{2}$ . Since the  $\mathbb{Z}_4$  parafermion theory is described by a free boson compactified on the  $S^1/\mathbb{Z}_2$  orbifold with  $r_{\text{PF}} = \sqrt{2/3}$  [25], the continuum limit of the XXZ $_{1/2}$  model with  $\alpha_{\text{PF}} = \frac{2}{3}\pi$  gives the  $\mathbb{Z}_4$  parafermions.

In terms of the XXZ $_{1/2}$  model, the chemical potential  $\mu = e^{i\phi}$  in the TBA equations is understood as the twist parameter of the boundary conditions [26–28],

$$S_{N+1}^z = S_1^z, \quad S_{N+1}^\pm = e^{\pm \frac{2}{3} i \phi} S_1^\pm. \quad (3.8)$$

The bosonization formula (3.7) means that these are equivalent to the winding condition on the dual boson [5, 29],  $\tilde{\Phi}(\tau, \sigma + R) \sim \tilde{\Phi}(\tau, \sigma) - \frac{4}{3r} \phi$ , where  $R$  is the length of the space. For the original boson  $\Phi$ , this induces the shift of the momenta,

$$\frac{n}{R} \rightarrow \frac{1}{R} \left( n - \frac{\phi}{3\pi r} \right) \quad (n \in \mathbb{Z}). \quad (3.9)$$

One can check that the ground state energy is also changed to (see also [30])

$$E_\Phi = -\frac{\pi}{6R} \left( 1 - \frac{2\phi^2}{3\pi(\pi - \alpha)} \right), \quad (3.10)$$

due to the momentum shift, and that the TBA result in [3] is indeed reproduced for  $\alpha = \alpha_{\text{PF}}$ :

$$E_0 = E_\Phi|_{\alpha=\alpha_{\text{PF}}} = -\frac{\pi}{6R} \left( 1 - \frac{2\phi^2}{\pi^2} \right). \quad (3.11)$$

The above discussion shows that the vacuum operator  $V$  for general  $\mu$  is identified with the momentum shift operator,

$$V = e^{-i\frac{\phi}{3\pi r} \Phi} = e^{-i\sqrt{\frac{\pi}{6}} \frac{\phi}{\pi} \Phi}, \quad (3.12)$$

when the parafermions are bosonized. The energy operator  $\varepsilon$  is also given simply by the vertex operators of  $\Phi$ , since it is in the untwisted sector of the  $S^1/\mathbb{Z}_2$  orbifold compactification. The conformal dimension then determines its bosonized form,

$$\varepsilon = a_+ e^{i\sqrt{\frac{2}{3}} \Phi} + a_- e^{-i\sqrt{\frac{2}{3}} \Phi}, \quad (3.13)$$



where  $a_{\pm}$  are some coefficients including cocycle factors. Their explicit forms can be found in [31] but, here, we only note that the products  $a_{\pm}a_{\mp}$  are c-numbers.

Now, we are ready to evaluate the expansion of the ground state energy  $E(R)$ . The first non-trivial term in (3.4) comes from the two-point function. Since  $\varepsilon$  is canonically normalized as  $\langle \varepsilon(z)\varepsilon(0) \rangle|_{\phi=0} = |z|^{-4/3}$ , one has for general  $\phi$

$$\begin{aligned} \left\langle \varepsilon(z_2)\varepsilon(z_1) \right\rangle_{\phi} &= \left\langle e^{i\sqrt{\frac{1}{6}\frac{\phi}{\pi}}\Phi(\infty)} e^{i\sqrt{\frac{2}{3}}\Phi(z_2)} e^{-i\sqrt{\frac{2}{3}}\Phi(z_1)} e^{-i\sqrt{\frac{1}{6}\frac{\phi}{\pi}}\Phi(0)} \right\rangle \\ &= |1 - z_2|^{-\frac{4}{3}} |z_2|^{\frac{2}{3\pi}\phi}, \end{aligned} \quad (3.14)$$

with  $z_1 = 1$ . The integral of this term is evaluated in (3.4) by the formula,

$$\int d^2u |u|^{2a} |1 - u|^{2b} = \pi \gamma(1+a) \gamma(1+b) \gamma(-1-a-b). \quad (3.15)$$

Collecting the results so far, we find the free energy near the CFT point to be

$$F = RE_0 + |Z|^2 - C_{\frac{8}{3}} \gamma\left(\frac{1}{3} + \frac{\phi}{3\pi}\right) \gamma\left(\frac{1}{3} - \frac{\phi}{3\pi}\right) |Z|^{\frac{8}{3}} + \mathcal{O}(|Z|^{\frac{16}{3}}), \quad (3.16)$$

where

$$C_{\frac{8}{3}} = \frac{\pi}{2} \left[ \frac{1}{\sqrt{\pi}} \gamma\left(\frac{3}{4}\right) \right]^{\frac{8}{3}} \gamma\left(\frac{1}{6}\right) \gamma\left(\frac{1}{3}\right) \approx 0.18461. \quad (3.17)$$

At  $\phi = \pi$  the coefficient of  $|Z|^{\frac{8}{3}}$  diverges, which implies that the CFT perturbation breaks down there. The expansions to higher orders are straightforward. Figure 4 and 5 show  $A_{\text{free}} = -F$  from the above CFT perturbation and the numerical computation. The results in (3.14) and (3.16) may be continued to imaginary  $\phi$ . While real  $\phi$  is physical in the context of the XXZ spin-chain, so is imaginary  $\phi$  in the context of thermodynamics. Note that imaginary  $\phi$  corresponds to minimal surfaces in (2, 2) signature [3].

#### 4. Remainder function around CFT point

The remainder function (2.52) essentially consists of two non-trivial functions,  $A_{\text{free}}$  and  $R_1$ . We studied the structure of  $A_{\text{free}}$  for  $|Z| \ll 1$  in the last section. Here let us see how  $R_1$  behaves as a function of  $|Z|, \varphi, \phi$  in the region  $|Z| \ll 1$ .

We know the form of  $R_1$  as a function of  $U_k$  (2.54). Using (2.36), one can express it in terms of Y-functions as

$$R_1 = -\frac{1}{4} \sum_{k=1}^3 \text{Li}_2 \left( -Y_2 \left( \frac{(2k+1)\pi i}{4} \right) \right). \quad (4.1)$$

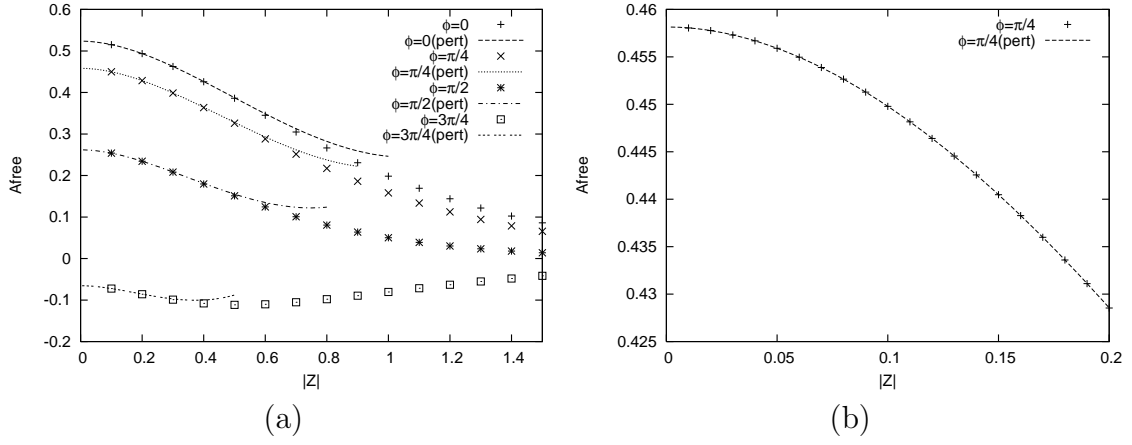


Figure 4: (a) Plots of  $(|Z|, A_{\text{free}})$  for various values of  $\phi$  at  $\varphi = -\pi/48$ . (b) Plots of  $(|Z|, A_{\text{free}})$  for  $0 \leq |Z| \leq 0.2$  at  $\phi = \pi/4$ ,  $\varphi = -\pi/48$ .

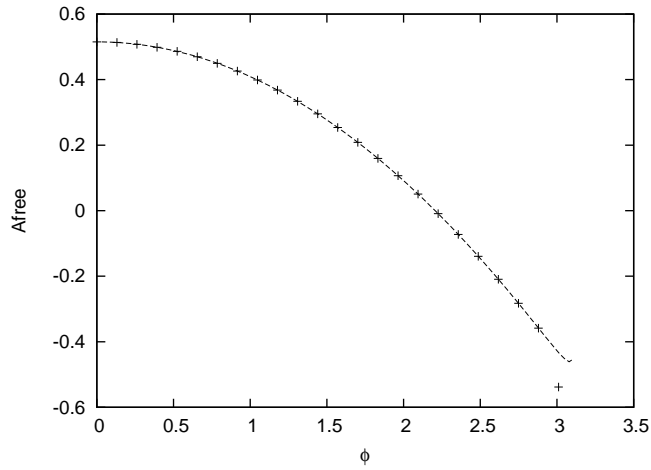


Figure 5: Plots of  $A_{\text{free}}$  for  $0 \leq \phi \leq \pi$  at  $|Z| = 0.1$  and  $\varphi = -\pi/48$ . The dashed line represents the graph calculated by the formula (3.16).

What we need is the information of how  $|Z|, \varphi, \phi$  enters in the function  $Y_2(\theta)$ . From (2.41)–(2.43) we see that  $\theta$  and  $\varphi$  appear in the Y-functions only through the combination  $\theta + i\varphi$ . The Y-functions are periodic in  $\theta$  (2.34) and also exhibit  $\mathbb{Z}_2$  symmetries (2.35), (2.47). Also they are regular everywhere except at  $\text{Re } \theta = \pm\infty$ , as we mentioned in section 2.5. Combining all these properties together, we see that the Y-functions admit the following Laurent expansion [11]

$$Y_a(\theta) = Y_a^{(0)}(|Z|, \phi) + \sum_{n=1}^{\infty} Y_a^{(n)}(|Z|, \phi)(t^n + t^{-n}), \quad t = e^{\frac{4}{3}(\theta - i\varphi)}, \quad (4.2)$$

where  $Y_a^{(n)} \in \mathbb{R}$ . By substituting this into the expression (4.1), one obtains the following Fourier expansion for  $R_1$

$$R_1 = \sum_{m=0}^{\infty} R_1^{(m)}(|Z|, \phi) \cos 4m\varphi. \quad (4.3)$$

Note that in deriving this expression, there occur cancellations among powers of  $t^n$  evaluated at  $\theta = (2k+1)\pi i/4$ ,  $k = 1, 2, 3$ , whenever  $n$  is not a multiple of 3. By construction the coefficients  $R_1^{(m)}$  are real. Therefore  $R_1$  has shown to be real-valued, even, periodic function in  $\varphi$  with periodicity  $\pi/2$ . Our numerical results indeed exhibit this periodicity.

Let us now analyze the form of  $R_1$  for  $|Z| \ll 1$ . It is seen from (2.42)–(2.43) that the Y-functions grow dramatically at large  $\theta$  but do not vary so much in the region  $-\log(1/|Z|) \ll \theta \ll \log(1/|Z|)$ . In other words, Y-functions draw a plateau over the region, which is wide when  $|Z|$  is small. In order for the Y-functions to be so, the coefficients  $Y_a^{(n)}$  in the expansion (4.2) have to be sufficiently small and at most

$$Y_a^{(n)}(|Z|, \phi) \sim |Z|^{\frac{4}{3}n} + (\text{higher order terms}). \quad (4.4)$$

The appearance of powers of  $|Z|^{4/3} = |U|$  is not totally unexpected, as we have already seen in the last section that the CFT result for  $A_{\text{free}}$  is obtained in powers of  $|Z|^{\frac{8}{3}}$ . This suggests us that the Y-functions, and thus their descendants  $U_k$  and  $R_1$ , may well be expanded in powers of  $|Z|^{4/3} = |U|$ . Below we assume that this is the case. Let us then express  $Y_2$  as

$$Y_2(\theta) = \sum_{n=0}^{\infty} \tilde{Y}_2^{(n)}(\varphi + i\theta, \phi) |Z|^{\frac{4}{3}n}. \quad (4.5)$$

The first coefficient is the value of  $Y_2$  evaluated at  $Z = 0$  and is known [3] as

$$\tilde{Y}_2^{(0)}(\varphi, \phi) = 1 + \mu^{2/3} + \mu^{-2/3} = 1 + 2 \cos \frac{2\phi}{3}. \quad (4.6)$$

(4.4) tells us that only the terms with  $n = 0, 1$  in (4.2) contribute to the next coefficient  $\tilde{Y}_2^{(1)}$ . Therefore  $\tilde{Y}_2^{(1)}$ , as a function of  $\varphi$ , is at most the sum of a term independent of  $\varphi$  and a term proportional to  $t + t^{-1} = 2\cos[4(\varphi + i\theta)/3]$ . As a matter of fact, the former term is not allowed by the Y-system relations (2.32), (2.33). Hence  $\tilde{Y}_2^{(1)}$  has to be of the form

$$\tilde{Y}_2^{(1)}(\varphi, \phi) = y^{(1)}(\phi) \cos \frac{4(\varphi + i\theta)}{3}. \quad (4.7)$$

This form is also confirmed by numerical computations. At present we do not know the analytic expression for the function  $y^{(1)}(\phi)$ , but it can be evaluated numerically as in Figure 6. Similarly,  $\tilde{Y}_2^{(2)}$  depends on  $\varphi$  only through  $\cos[4(\varphi + i\theta)/3]$  and  $\cos[8(\varphi + i\theta)/3]$ , but actually we do not need the precise form here. By using the above data and the Y-system relations (2.32)–(2.33), one can determine the behavior of  $R_1$  for  $|Z| \ll 1$ . If we express  $R_1$  in the form

$$R_1 = \sum_{n=0}^{\infty} \tilde{R}_1^{(n)}(\varphi, \phi) |Z|^{\frac{4}{3}n}, \quad (4.8)$$

the first few coefficients are obtained as

$$\tilde{R}_1^{(0)}(\varphi, \phi) = -\frac{3}{4} \text{Li}_2(1 - 4\beta^2), \quad (4.9)$$

$$\tilde{R}_1^{(1)}(\varphi, \phi) = 0, \quad (4.10)$$

$$\tilde{R}_1^{(2)}(\varphi, \phi) = \frac{3(4\beta^2 - 1 + \log(4\beta^2))}{64\beta^2(4\beta^2 - 1)^2} y^{(1)}(\phi)^2, \quad (4.11)$$

with  $\beta = \cos(\phi/3)$ . Note that these three coefficients are  $\varphi$ -independent. This is consistent with the argument below (4.3) that Fourier modes  $\cos(4n\varphi/3)$  with  $n$  not being a multiple of 3 cancel out in  $R_1$ . The  $\varphi$ -dependence could start appearing at the order of  $|Z|^4$ . The above result agrees with numerical computation with high accuracy. Figure 7 shows a comparison between the above perturbative approximation with numerical plots.

Collecting the results so far, the remainder function is expanded around  $|Z| = 0$  as

$$\begin{aligned} R = & - \left[ \frac{\pi}{6} \left( 1 - \frac{2\phi^2}{\pi^2} \right) + \frac{3}{4} \text{Li}_2(1 - 4\beta^2) \right] \\ & + \left[ -C_{\frac{8}{3}} \gamma \left( \frac{1}{3} + \frac{\phi}{3\pi} \right) \gamma \left( \frac{1}{3} - \frac{\phi}{3\pi} \right) + \frac{3(4\beta^2 - 1 + \log(4\beta^2))}{64\beta^2(4\beta^2 - 1)^2} y^{(1)}(\phi)^2 \right] |Z|^{\frac{8}{3}} \\ & + \mathcal{O}(|Z|^4). \end{aligned} \quad (4.12)$$

Note that  $|Z|^2$  terms in  $A_{\text{periods}}$  and in  $A_{\text{free}}$  cancel each other. Figure 8 shows a comparison between the perturbative approximation with numerical plots.

One can also express the cross-ratios  $U_k$  ( $k = 1, 2, 3$ ) as

$$U_k = 4\beta^2 + y^{(1)}(\phi) \left( \cos \frac{4\varphi - (2k+1)\pi}{3} \right) |Z|^{\frac{4}{3}} + \mathcal{O} \left( |Z|^{\frac{8}{3}} \right). \quad (4.13)$$

These are inverted to express  $|Z|, \varphi, \phi$  as functions of  $U_k$ :

$$\beta^2 = \cos^2 \frac{\phi}{3} = \frac{1}{12}(U_1 + U_2 + U_3), \quad (4.14)$$

$$\tan \frac{4}{3}\varphi = \frac{\sqrt{3}(U_2 - U_3)}{2U_1 - U_2 - U_3}, \quad (4.15)$$

$$|Z|^{\frac{4}{3}} = \frac{-2U_1 + U_2 + U_3}{3y^{(1)}(\phi) \cos \frac{4}{3}\varphi}. \quad (4.16)$$

With help of numerical fitting,  $y^{(1)}$  is also evaluated, *e.g.*, as (see Figure 6)

$$\begin{aligned} y^{(1)}(\phi) &\approx 5.47669 - 0.484171\phi^2 + 0.0119471\phi^2 \\ &\approx 1.31367 + 2.61136 \cos \frac{\phi}{3} + 1.55402 \cos \frac{2\phi}{3}. \end{aligned} \quad (4.17)$$

Substituting these into (4.12) gives an analytic expansion of  $R$  in terms of  $U_k$ , which can be directly compared with weak coupling results. This expansion describes the behavior of  $R$  around the locus  $U_1 = U_2 = U_3$ .

One can check that the Jacobian of the above change of variables is proportional to  $(y^{(1)})^2 |Z|^{\frac{5}{3}} \sin(\frac{2}{3}\phi)$  and the transformation is one-to-one for  $|Z| \neq 0$ ,  $0 \leq \varphi < 3\pi/2$  and  $0 < \phi < 3\pi/2$ . The range of  $\varphi$  comes from that of the phase of  $U$  as seen in (2.40), while the range of  $\phi$  corresponds to the region where minimal surfaces are in (1, 3) and usual (3, 1) signatures [3]. From (4.13), one also finds that all  $(|Z|, \varphi, \phi)$  near the CFT point correspond to real cross-ratios. In the above approximation, each of  $|Z|, \varphi, \phi$  has the following geometrical meaning in the parameter space  $(U_1, U_2, U_3)$ : (4.14) implies that constant  $\phi$  spans a plane perpendicular to the locus  $U_1 = U_2 = U_3$ .  $\phi$  specifies the distance between the plane and the origin. On this plane,  $\varphi$  parametrizes a circle around the center  $U_1 = U_2 = U_3 = 4\beta^2$  with a radius of  $\sqrt{3/2} y^{(1)}(\phi) |Z|^{4/3}$ . Thus, in terms of the cross-ratios, the weak dependence of  $R$  on  $\varphi$  for small  $|Z|$  observed above is translated into that on the rotation around the locus  $U_1 = U_2 = U_3$ .

## 5. Remainder function in large mass region

So far, we have studied the remainder function when the mass scale  $|Z|$  is small. In this section, following [12] we consider the large mass region, *i.e.*,  $|Z| \gg 1$ , which

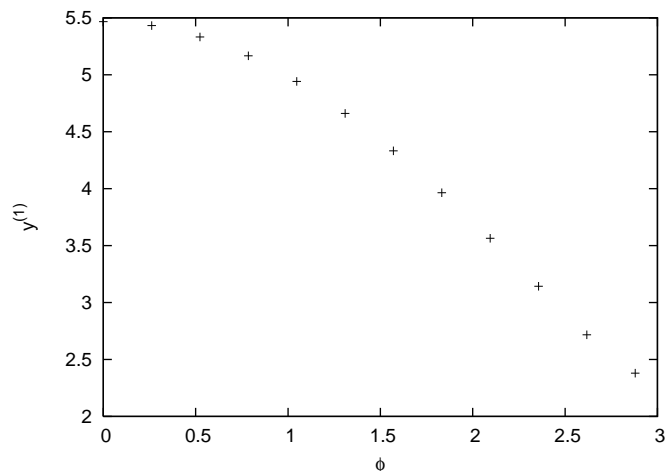


Figure 6: Plots of  $y^{(1)}(\phi)$  obtained by fitting the numerical data of  $Y_2(\theta)$  in the region  $0.01 \leq |Z| \leq 0.2$  at  $\varphi = -\pi/48$ . When we fit the numerical data of  $y^{(1)}(\phi)$  by the function  $a + b\phi^2 + c\phi^4$ , we find that the coefficients are given by  $a = 5.47669$ ,  $b = -0.484171$ ,  $c = 0.0119471$ . If we fit them by  $\tilde{a} + \tilde{b} \cos(\phi/3) + \tilde{c} \cos(2\phi/3)$ , we obtain  $\tilde{a} = 1.31367$ ,  $\tilde{b} = 2.61136$ ,  $\tilde{c} = 1.55402$ .

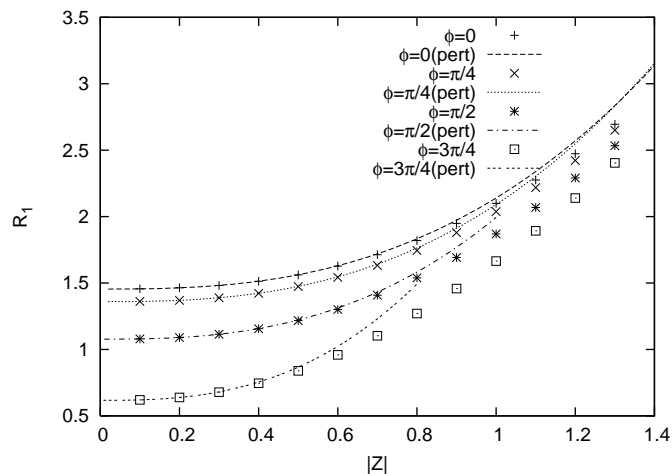


Figure 7: Numerical plots of  $|Z| - R_1$  vs perturbative solution of  $R_1$  at  $\varphi = -\pi/48$ . Here we use  $y^{(1)}(\phi)$  in Figure 6.

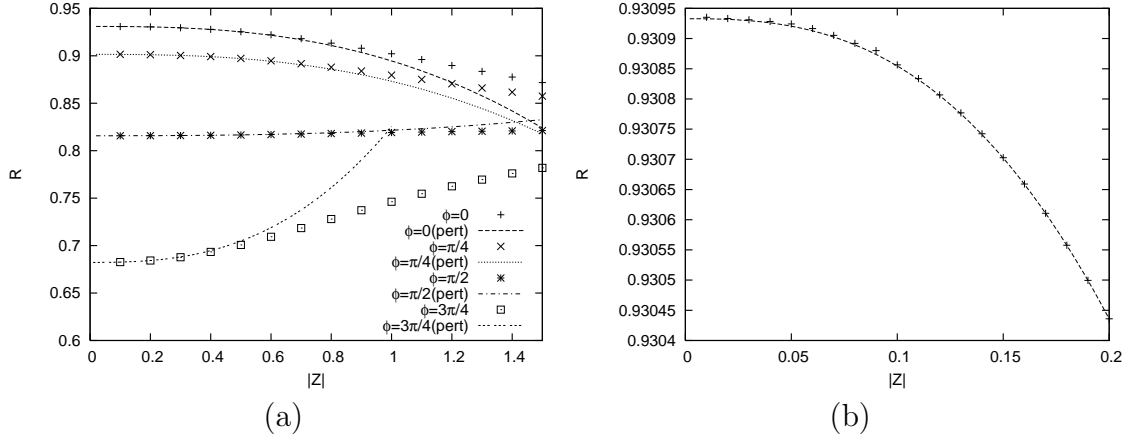


Figure 8: Numerical plots of  $|Z|-R$  vs perturbative solution of  $R$  (a) for various values of  $\phi$  at  $\varphi = -\pi/48$  (b) in the region  $0 \leq |Z| \leq 0.2$  at  $\phi = 0$  and  $\varphi = -\pi/48$ .

corresponds to the kinematical region around collinear limits. In this region, we can solve the TBA equations approximately. Throughout this section, we consider the case that  $-\pi/4 < \varphi < 0$ . Other cases can be analyzed similarly by using (2.48), (2.49).

Let us first consider the free energy. For large  $|Z|$ , the pseudo-energies,  $\epsilon$ ,  $\tilde{\epsilon}$ , behave as  $\epsilon(\theta) \approx 2|Z| \cosh \theta$  and  $\tilde{\epsilon}(\theta) \approx 2\sqrt{2}|Z| \cosh \theta$ . The convolution terms in the TBA equations are suppressed exponentially. Thus the free energy is evaluated by

$$A_{\text{free}} \approx \int_{-\infty}^{\infty} \frac{d\theta}{2\pi} \left[ (\mu + \mu^{-1}) 2|Z| \cosh \theta e^{-2|Z| \cosh \theta} + 2\sqrt{2}|Z| \cosh \theta e^{-2\sqrt{2}|Z| \cosh \theta} \right]. \quad (5.1)$$

One can easily find that the free energy is expressed in terms of the modified Bessel function of the second kind,

$$A_{\text{free}} \approx \frac{2|Z|}{\pi} \left[ (\mu + \mu^{-1}) K_1(2|Z|) + \sqrt{2} K_1(2\sqrt{2}|Z|) \right]. \quad (5.2)$$

From the asymptotics of the modified Bessel function we see that  $A_{\text{free}}$  decays exponentially as  $|Z|$  goes to  $\infty$ .

Next, let us consider the large  $|Z|$  behavior of  $R_1$ . The leading correction of  $b_1$  is given by

$$b_1 = e^{\epsilon(-i\varphi)} \approx e^{2|Z| \cos(\hat{\varphi} - \pi/4)} (1 + \delta_1), \quad (5.3)$$

where  $\hat{\varphi} \equiv \varphi + \pi/4$  and

$$\delta_1 \equiv \int_{-\infty}^{\infty} d\theta \left[ \mathcal{K}_2 \left( i\hat{\varphi} - \frac{\pi i}{4} + \theta \right) e^{-2\sqrt{2}|Z| \cosh \theta} + (\mu + \mu^{-1}) \mathcal{K}_1 \left( i\hat{\varphi} - \frac{\pi i}{4} + \theta \right) e^{-2|Z| \cosh \theta} \right]. \quad (5.4)$$

The kernels are defined in (2.44). Similarly,

$$U_2 - 1 = e^{\tilde{c}(-i\hat{\varphi})} \approx e^{2\sqrt{2}|Z| \cos \hat{\varphi}} (1 + \delta_2) \quad (5.5)$$

with

$$\delta_2 \equiv \int_{-\infty}^{\infty} d\theta \left[ 2\mathcal{K}_1(i\hat{\varphi} + \theta) e^{-2\sqrt{2}|Z| \cosh \theta} + (\mu + \mu^{-1}) \mathcal{K}_2(i\hat{\varphi} + \theta) e^{-2|Z| \cosh \theta} \right]. \quad (5.6)$$

From these and (2.37), (2.38), we can compute  $b_2$  and  $b_3$ ,

$$b_3 = \frac{U_2}{b_1} = e^{2|Z| \cos(\hat{\varphi} + \pi/4)} (1 + \delta_3), \quad b_2 = \frac{b_1 + b_3 + \mu + \mu^{-1}}{b_1 b_3 - 1}, \quad (5.7)$$

where

$$\delta_3 \equiv \frac{\delta_2 - \delta_1 + e^{-2\sqrt{2}|Z| \cos \hat{\varphi}}}{1 + \delta_1}. \quad (5.8)$$

Thus the other cross-ratios  $U_1$  and  $U_3$  are given by

$$1 - U_1 = 1 - b_2 b_3 = -e^{-2\sqrt{2}|Z| \sin \hat{\varphi}} (1 + \Delta_1), \quad (5.9)$$

$$1 - U_3 = 1 - b_1 b_2 = -e^{2\sqrt{2}|Z| \sin \hat{\varphi}} (1 + \Delta_3), \quad (5.10)$$

with

$$\Delta_1 \equiv \frac{(1 + \delta_3 + \mu e^{-2|Z| \cos(\hat{\varphi} + \pi/4)})(1 + \delta_3 + \mu^{-1} e^{-2|Z| \cos(\hat{\varphi} + \pi/4)})}{1 + \delta_2} - 1, \quad (5.11)$$

$$\Delta_3 \equiv \frac{(1 + \delta_1 + \mu e^{-2|Z| \cos(\hat{\varphi} - \pi/4)})(1 + \delta_1 + \mu^{-1} e^{-2|Z| \cos(\hat{\varphi} - \pi/4)})}{1 + \delta_2} - 1. \quad (5.12)$$

Note that all  $\delta_i$  and  $\Delta_i$  decay exponentially as  $|Z|$  goes to  $\infty$ .

Here let us give a comment on the large  $|Z|$  behaviors of the cross-ratios. When  $\hat{\varphi}$  is far from zero, the cross-ratios show the asymptotic behavior  $(u_1, u_2, u_3) \rightarrow (1, 0, 0)$  as  $|Z| \rightarrow \infty$  where  $u_k \equiv 1/U_k$  ( $k = 1, 2, 3$ ). However if  $\hat{\varphi}$  approaches zero,  $(u_1, u_2, u_3)$  can reach an arbitrary point on the segment  $(1 - c, 0, c)$  ( $0 < c < 1/2$ ). To see this, we need to take the double scaling limit  $\hat{\varphi} \rightarrow +0, |Z| \rightarrow \infty$  with  $|Z| \sin \hat{\varphi} = a (> 0)$  held fixed. In this limit the cross-ratios go to the point (see Figure 9)

$$(u_1, u_2, u_3) \rightarrow (1/(1 + e^{-2\sqrt{2}a}), 0, 1/(1 + e^{2\sqrt{2}a})). \quad (5.13)$$



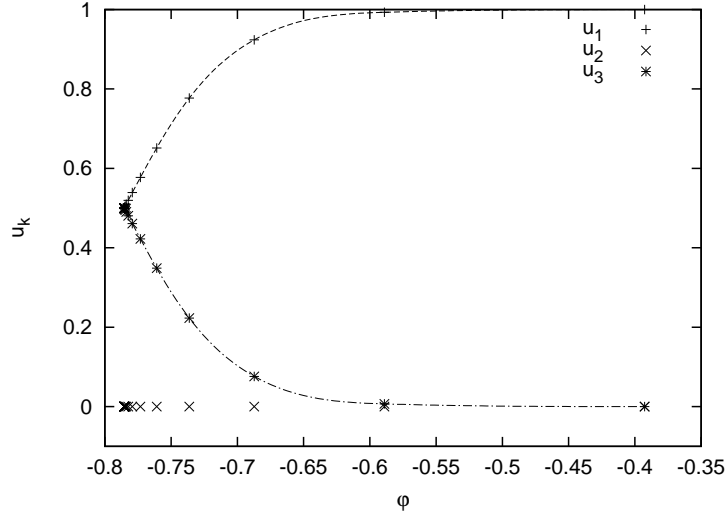


Figure 9: We take a large value  $|Z| = 9.0$  and plot the value of  $u_k (= 1/U_k)$  for various  $\varphi$  at fixed  $\phi = 0$ . Dashed lines correspond to the formula (5.13) obtained by taking the collinear limit.

In order to invert the relation between  $(|Z|, \varphi, \phi)$  and the cross-ratios for large  $|Z|$ , one has to evaluate the integrals in (5.4) and (5.6) in more detail.

To analyze the large  $|Z|$  behavior of  $R_1$ , the following asymptotic expansion is useful:

$$\text{Li}_2(-e^x(1+\delta)) = -\frac{x^2}{2} - \frac{\pi^2}{6} - x\delta + e^{-x} + \mathcal{O}(\delta^2, e^{-x}\delta, e^{-2x}) \quad (x \gg 1 \text{ and } \delta \ll 1). \quad (5.14)$$

Therefore the asymptotic behavior of  $R_1$  is given by

$$R_1 \approx |Z|^2 + \frac{\pi^2}{12} + \frac{1}{4}(2\sqrt{2}|Z| \cos \hat{\varphi} \delta_2 + 2\sqrt{2}|Z| \sin \hat{\varphi} \Delta_3 - e^{-2\sqrt{2}|Z| \cos \hat{\varphi}} + e^{-2\sqrt{2}|Z| \sin \hat{\varphi}} \Delta_1). \quad (5.15)$$

The first term is divergent in the large  $|Z|$  limit, but this term is canceled by the second term in (2.52). Combining all the above results, we finally arrive at the large mass behavior of the remainder function

$$R \approx \frac{\pi^2}{12} - \frac{2|Z|}{\pi} \left[ (\mu + \mu^{-1}) K_1(2|Z|) + \sqrt{2} K_1(2\sqrt{2}|Z|) \right] + \frac{1}{4}(2\sqrt{2}|Z| \cos \hat{\varphi} \delta_2 + 2\sqrt{2}|Z| \sin \hat{\varphi} \Delta_3 - e^{-2\sqrt{2}|Z| \cos \hat{\varphi}} + e^{-2\sqrt{2}|Z| \sin \hat{\varphi}} \Delta_1). \quad (5.16)$$

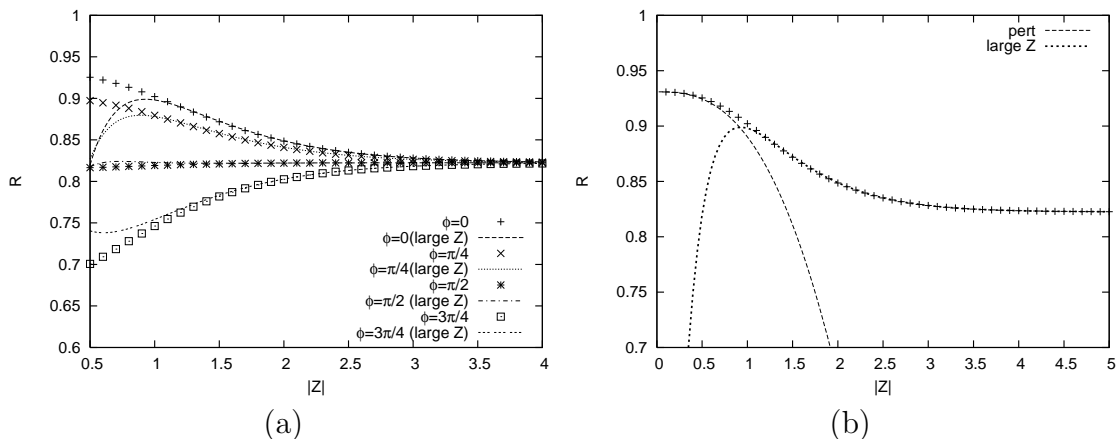


Figure 10: (a) Large  $|Z|$  behavior of the remainder function for various  $\phi$  at  $\hat{\varphi} = 5\pi/24$ . Dashed lines show the asymptotic expansion obtained by (5.2) and (5.15). Points show the numerical results. (b) The  $|Z|$ -dependence of the remainder function vs the small (dashed line) and the large (dotted line)  $|Z|$  expansions at  $\phi = 0$  and  $\varphi = -\pi/48$ . The two expansions cover the whole region in  $|Z|$  except a small region around  $|Z| = 1.0$ .

where  $\delta_2$ ,  $\Delta_1$  and  $\Delta_3$  are given by (5.6), (5.11) and (5.12) respectively. Since the second and the third terms decay exponentially to zero in the large mass limit, the remainder function approaches the constant  $\pi^2/12$ .

Figure 10 shows the behavior of the remainder function in the large  $|Z|$  limit. For the large  $|Z|$ , the asymptotic expansion of the remainder function (5.16) is in good agreement with the numerical data. Figure 11 shows the  $\hat{\varphi}$ -dependence of the remainder function for the large  $|Z|$ . We observe that  $\hat{\varphi}$ -dependence is weak. This can also be seen in the analytic form (5.16) where the  $\hat{\varphi}$ -dependence is suppressed exponentially in  $|Z|$ .

## 6. Conclusions

In this paper we have studied the remainder function of 6-point gluon scattering amplitudes in  $\mathcal{N} = 4$  super Yang–Mills theory by analyzing the TBA equations perturbatively and numerically. We have examined perturbative solution near the UV and IR limits and found that results are consistent with the numerical results. The remainder function is made of the free energy of the  $\mathbb{Z}_4$ -symmetric integrable model and the difference between the BDS part and the BDS-like part. The free energy near the CFT point can be obtained by the correlation functions with the chemical potential background. It is an interesting problem to generalize this result

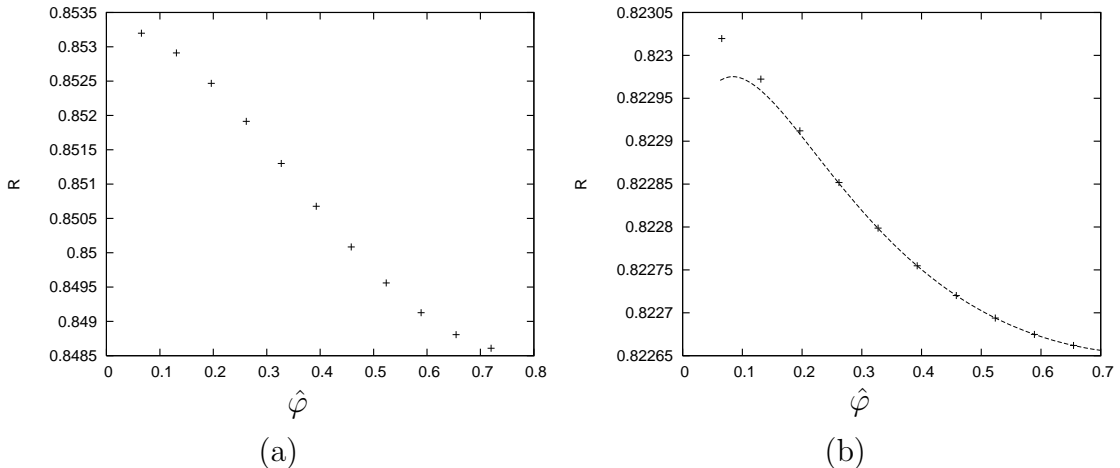


Figure 11:  $\hat{\phi}$ -dependence of the remainder function (a) at  $|Z| = 2.0$  and  $\phi = 0$  and (b) at  $|Z| = 5.0$  and  $\phi = 0$ . The dashed line and points correspond to the asymptotic expansion and the numerical results, respectively. We see that  $R$  does not depend very much on  $\hat{\phi}$ . ( $R$  varies only up to 0.6% at  $|Z| = 2.0$  and 0.05% at  $|Z| = 5.0$ .)

to the case of  $n$ -point amplitudes corresponding to the generalized parafermions. The other part of the remainder function  $R_1$  is written as the sum of the dilogarithm function including Y-functions as arguments. In the present work, we could not completely determine its analytic form near the CFT point, but the undermined function of the chemical potential has been evaluated by numerical fitting. It is also an interesting problem to determine the series expansions of the Y-functions in order to know analytical properties of the remainder functions. In the large mass limit, we have obtained the first order correction to the remainder function. It would be useful to apply nonlinear integral equation approach [32] to analyze the TBA system further.

Our results provide an analytic form of the remainder function for the 6-point amplitude at strong coupling away from the UV(CFT) and the IR(collinear) point. Such an analytic form beyond numerical ones will be important for further studying the super Yang–Mills theory at strong coupling. In particular, together with the recent results of the analytic form at weak coupling [33, 34], which is still under active investigation, our strong coupling result will give a clue to understand the scattering amplitude to all order in the context of the AdS/CFT correspondence. In this regard, comparisons with the perturbative (both analytic and numerical) computations [10, 33–35] would be of interest. One can expect that the physical picture of the amplitude to all order will emerge through further investigations both

at weak and strong coupling. As shown in Figure 10, we also find that simple first order expansions away from the UV and IR points give a good approximation to the remainder function for all the scale  $|Z|$  as long as the expansions are valid. In addition, our results demonstrate that the identification of the two-dimensional integrable models underlying the four-dimensional super Yang–Mills theory [3, 6] is useful, as well as interesting, for actual computations of the amplitude at strong coupling. The discussion in this paper may also be generalized to other TBA systems with chemical potential.

The free energy  $A_{\text{free}}$  is independent of  $\varphi$ , the phase of  $Z$ . From perturbative and numerical analysis, we observe that the  $\varphi$ -dependence of the remainder function is also weak: it starts appearing possibly at the order of  $|Z|^4$  for small  $|Z|$  and at the order of  $e^{-c|Z|}$  with  $c$  being some positive constant for large  $|Z|$ . In terms of the cross-ratios  $U_k$ , the weak dependence for small  $|Z|$  is translated into that on the rotation around the locus  $U_1 = U_2 = U_3$ . It would be important to further investigate the meaning of the  $\varphi$ -dependence to explore quantum corrections to the present analysis as noted in [5].

### Acknowledgments

We would like to thank J. Suzuki for useful discussions. Y. S. would like to thank J. Balog for useful discussions and conversations. The work of K. S. and Y. S. is supported in part by Grant-in-Aid for Scientific Research from the Japan Ministry of Education, Culture, Sports, Science and Technology.

### References

- [1] L. F. Alday and J. M. Maldacena, JHEP **0706** (2007) 064 [arXiv:0705.0303 [hep-th]].
- [2] L. F. Alday and J. Maldacena, JHEP **0911** (2009) 082 [arXiv:0904.0663 [hep-th]].
- [3] L. F. Alday, D. Gaiotto and J. Maldacena, arXiv:0911.4708 [hep-th].
- [4] B. A. Burrington and P. Gao, JHEP **1004** (2010) 060 [arXiv:0911.4551 [hep-th]].
- [5] L. F. Alday, J. Maldacena, A. Sever and P. Vieira, arXiv:1002.2459 [hep-th].

- [6] Y. Hatsuda, K. Ito, K. Sakai and Y. Satoh, JHEP **1004** (2010) 108 [arXiv:1002.2941 [hep-th]].
- [7] G. Yang, arXiv:1004.3983 [hep-th].
- [8] Z. Bern, L. J. Dixon and V. A. Smirnov, Phys. Rev. D **72**, 085001 (2005) [arXiv:hep-th/0505205].
- [9] L. F. Alday and J. Maldacena, JHEP **0711** (2007) 068 [arXiv:0710.1060 [hep-th]].
- [10] J.M. Drummond, J. Henn, G.P. Korchemsky and E. Sokatchev, Nucl. Phys. B **815** (2009) 142 [arXiv:0803.1466[hep-th]];  
Z. Bern, L.J. Dixon, D.A. Kosower, R. Roiban, M. Spradlin, C. Vergu and A. Volovich, Phys. Rev. D **78** (2008) 045007 [arXiv:0803.1465[hep-th]].
- [11] A. B. Zamolodchikov, Phys. Lett. B **253** (1991) 391.
- [12] Al. B. Zamolodchikov, Nucl. Phys. B **342** (1990) 695.
- [13] R. Koberle and J. A. Swieca, Phys. Lett. B **86** (1979) 209.
- [14] A. M. Tsvetick, Nucl. Phys. B **305** [FS23] (1988) 675.
- [15] V. A. Fateev, Int. J. Mod. Phys. A **6** (1991) 2109.
- [16] C. R. Fernandez-Pousa, M. V. Gallas, T. J. Hollowood and J. L. Miramontes, Nucl. Phys. B **484** (1997) 609 [arXiv:hep-th/9606032]; Nucl. Phys. B **499** (1997) 673 [arXiv:hep-th/9701109].
- [17] V. A. Fateev and A. B. Zamolodchikov, Sov. Phys. JETP **62** (1985) 215 [Zh. Eksp. Teor. Fiz. **89** (1985) 380];  
D. Gepner and Z. Qiu, Nucl. Phys. B **285** (1987) 423;  
D. Gepner, Nucl. Phys. B **290** (1987) 10.
- [18] T. R. Klassen and E. Melzer, Nucl. Phys. B **338** (1990) 485;  
T. R. Klassen and E. Melzer, Nucl. Phys. B **350** (1991) 635.
- [19] K. Pohlmeyer, Commun. Math. Phys. **46** (1976) 207;  
H. J. De Vega and N. G. Sanchez, Phys. Rev. D **47** (1993) 3394.
- [20] P. Dorey, C. Dunning and R. Tateo, J. Phys. A **40** (2007) R205 [arXiv:hep-th/0703066].
- [21] D. Gaiotto, G. W. Moore and A. Neitzke, arXiv:0907.3987 [hep-th].
- [22] V. A. Fateev, Phys. Lett. B **324** (1994) 45.
- [23] I. Affleck, “Field theory methods and quantum critical phenomena,” in *Fields, strings and critical phenomena*, edited by E. Brezin and J. Zinn-Justin (North-Holland, Amsterdam, 1990).

- [24] A. Luther and I. Peschel, Phys. Rev. B **12** (1975) 3908.
- [25] S. K. Yang, Nucl. Phys. B **285** (1987) 639.
- [26] J. Suzuki, private communication.
- [27] A. Klumper, M. T. Batchelor and P. A. Pearce, J. Phys. A **24** (1991) 3113.
- [28] P. Fendley, Adv. Theor. Math. Phys. **1** (1998) 210 [arXiv:hep-th/9706161];  
P. Fendley and H. Saleur, arXiv:hep-th/9310058.
- [29] T. Nassar and O. Tirkkonen, J. Phys. A **31** (1998) 9983  
[arXiv:hep-th/9707098].
- [30] C. J. Hamer, G. R. W. Quispel and M. T. Batchelor, J. Phys. A **20** (1987)  
5677.
- [31] P. C. Argyres, E. Lyman and S. H. H. Tye, Phys. Rev. D **46** (1992) 4533  
[arXiv:hep-th/9205113].
- [32] P. A. Pearce and A. Klümper, Phys. Rev. Lett. **66** (1991) 974;  
C. Destri and H. J. de Vega, Phys. Rev. Lett. **69** (1992) 2313.
- [33] V. Del Duca, C. Duhr and V. A. Smirnov, JHEP **1003** (2010) 099  
[arXiv:0911.5332 [hep-ph]].
- [34] J. H. Zhang, arXiv:1004.1606 [hep-th].
- [35] C. Anastasiou, A. Brandhuber, P. Heslop, V. V. Khoze, B. Spence and  
G. Travaglini, JHEP **0905** (2009) 115 [arXiv:0902.2245 [hep-th]];  
A. Brandhuber, P. Heslop, V. V. Khoze and G. Travaglini, JHEP **1001** (2010)  
050 [arXiv:0910.4898 [hep-th]].